

## Age-related decrease in stimulated glutamate release and vesicular glutamate transporters in APP/PS1 transgenic and wild-type mice

R. Minkeviciene,\* J. Ihalainen,\* T. Malm,\* O. Matilainen,\* V. Keksa-Goldsteine,\* G. Goldsteins,\* H. Iivonen,\* N. Leguit,† J. Glennon,†‡ J. Koistinaho,\* P. Banerjee§ and H. Tanila\*¶

\**A.I. Virtanen Institute for Molecular Sciences, University of Kuopio, Finland*

†*Solvay Pharmaceuticals Research Laboratories, Weesp, Netherlands*

‡*Department of Chemistry, NUI Maynooth, Co. Kildare, Ireland*

§*Forest Laboratories, Jersey City, New Jersey, USA*

¶*Department of Neurology, Kuopio University Hospital, Kuopio, Finland*

### Abstract

We assessed baseline and KCl-stimulated glutamate release by using microdialysis in freely moving young adult (7 months) and middle-aged (17 months) transgenic mice carrying mutated human amyloid precursor protein and presenilin genes (APdE9 mice) and their wild-type littermates. In addition, we assessed the age-related development of amyloid pathology and spatial memory impaired in the water maze and changes in glutamate transporters. APdE9 mice showed gradual spatial memory impairment between 6 and 15 months of age. The stimulated glutamate release declined very robustly in 17-month-old APdE9 mice as compared to 7-month-old APdE9 mice. This age-dependent decrease in stimulated glutamate

release was also evident in wild-type mice, although it was not as robust as in APdE9 mice. When compared to individual baselines, all aged wild-type mice showed 25% or greater increase in glutamate release upon KCl stimulation, but none of the aged APdE9 mice. There was an age-dependent decline in VGLUT1 levels, but not in the levels of VGLUT2, GLT-1 or synaptophysin. Astrocyte activation as measured by glial acidic fibrillary protein was increased in middle-aged APdE9 mice. Blunted pre-synaptic glutamate response may contribute to memory deficit in middle-aged APdE9 mice.

**Keywords:** Alzheimer's disease, cortex, hippocampus, microdialysis, spatial memory.

*J. Neurochem.* (2007) 10.1111/j.1471-4159.2007.05147.x

Synaptic dysfunction is increasingly viewed as an early manifestation of Alzheimer's disease (AD) and a major correlate of cognitive impairment (Terry *et al.* 1991). While cholinergic depletion is an established hallmark in AD (Davies and Maloney 1976) and also detected in amyloid producing transgenic amyloid precursor protein (APP) mutant mice (Wong *et al.*, 1999), less is known about changes in glutamatergic neurotransmission. Since currently available therapies for AD include, in addition to cholinesterase inhibitors, the NMDA receptor partial antagonist memantine, more information about AD-related changes in glutamate neurotransmission would be highly relevant to better understand its mechanisms of action and to optimize the treatment. Several studies have reported reduced tissue levels of glutamate in the brains of AD patients (Hyman *et al.* 1987; Lowe *et al.* 1990), and a recent post-mortem study in AD patients found a reduction in the proteins levels

of vesicular glutamate transporter 1 (VGLUT1) in both the parietal and occipital cortices (Kirvell *et al.* 2006). On the other hand, glutamate-mediated excitotoxicity has been suggested to contribute to observed neuronal loss in AD

Received October 23, 2007; revised manuscript received November 19, 2007; accepted November 20, 2007.

Address correspondence and reprint requests to Heikki Tanila, MD, PhD, Professor in Molecular Neurobiology, Department of Neurobiology, A. I. Virtanen Institute, University of Kuopio, P.O. Box 1627/ Neulaniementie 2, 70211 Kuopio, Finland. E-mail: Heikki.Tanila@uku.fi

**Abbreviations used:** A $\beta$ ,  $\beta$ -amyloid; APP, amyloid precursor protein; APdE9, APP<sup>swe</sup>/PS1<sup>dE9</sup>; EAAT, excitatory amino acid transporter; GFAP, glial acidic fibrillary protein; GLT-1, glial glutamate transporter 1; GluR1, glutamate receptor subunit 1; NMDA, N-methyl-D-aspartic acid; PSI, presenilin-1; PSD-95, post-synaptic density protein with molecular weight of 95 kD; TTX, tetrodotoxin; VLUT, vesicular glutamate transporter.

(Greenamyre and Young 1989). In support of this notion, there are reports of reduced levels of excitatory amino acid transporter protein 1 (EAAT-1) in the platelets (Zoia *et al.* 2004) and EAAT-2 in the frontal cortex (Li *et al.* 1997), and reduced glutamate uptake activity in the frontal and temporal cortices of AD brains (Procter *et al.* 1988), which may lead to elevated extracellular glutamate concentration and render neurons for excitotoxicity.

Surprisingly, few studies to date have addressed the effect of beta-amyloid (A $\beta$ ) on glutamatergic synapses in experimental models. Studies in cultured hippocampal neurons (transfected or derived from APPswe mutant mice) have reported significant alternations in post-synaptic compartments because of beta-amyloid (A $\beta$ ) accumulation, including reduced spine density, and number of PSD-95 and GluR1 receptor levels (Almeida *et al.* 2005; Hsieh *et al.* 2006). Pre-synaptic changes were less pronounced but the levels of the pre-synaptic marker synaptophysin were lower in cells derived from APPswe mutant mice (Almeida *et al.* 2005). Dysregulation of glutamate receptors has also been found *in vivo* in APPswe mutant mice, albeit the change was an age-related increase in alpha-amino-3-hydroxy-5-methyl-4-isoxazole propionic acid (AMPA) receptor binding (Cha *et al.* 2001). Only one study to our knowledge has assessed structural alterations in glutamate terminals in APP mutant mice, and reported increased density of glutamatergic pre-synaptic boutons in both the plaque free and plaque adjacent cortical areas of 4-month-old transgenic mice as compared to non-transgenic controls (Bell *et al.* 2003). The authors interpreted the increased bouton size around plaques as an early stage of pathology, since cholinergic boutons show first increase in size followed by a later shrinkage. Thus the functional implication of the finding may be an increase in glutamate release early in amyloid pathology followed by a decreased release. Finally, only one study so far has assessed possible changes in glutamate transported levels in APP transgenic mice. This study (Masliah *et al.* 2000) reported a decrease in glial glutamate transporters, glutamate aspartate transporter (similar to human EAAT-1) and GLT-1 (similar to human EAAT-2), which may indicate elevated extracellular glutamate levels in these mice.

To determine the effects of A $\beta$  accumulation on glutamate release *in vivo*, we measured glutamate release in transgenic mice expressing human mutated APPswe and PS1(dE9) proteins (APdE9 mice) and their wild-type littermates at a young adult age (7 months) and in the middle-age (17 months). These mice exhibit first signs of amyloid plaque deposition at 3–4 months of age, although learning impairment occurs only between 12–19 months (Savonenko *et al.* 2005), suggesting additional non-amyloid factors responsible for learning impairment. Therefore, we first screened APdE9 mice for their spatial learning ability at 6, 10 and 15 months to get a better view of the time course of the development of memory impairment. In addition, recently

we reported reduced levels of vesicular acetylcholine transporter in the same mice at 7 months of age, with advanced reduction of cholinergic synaptic markers by 17 months of age (Machova *et al.* 2006), providing an interesting reference to possible glutamatergic synaptic changes in the same mouse model. Therefore, we selected 7 and 17 months as ages for the assay of extracellular glutamate levels using *in vivo* microdialysis. We also determined brain levels of A $\beta$ 40 and A $\beta$ 42 (both soluble and insoluble fractions), protein levels of the most important cortical and hippocampal vesicular glutamate transporters VGLUT1 and VGLUT2, as well as synaptophysin to assess synaptic integrity. In addition, we measured protein levels of the most important glutamate transporter in astrocytes GLT-1 and assessed relative number of activated astrocytes using glial acidic fibrillary protein (GFAP).

We found no evidence of increased extracellular glutamate levels in APdE9 mice, but a significant age-dependent decrease in stimulated glutamate release and a decrease in VGLUT1 levels in the hippocampus of both aged APdE9 and wild-type mice. More specifically, all aged APdE9 mice were completely resistant to stimulation-induced release of glutamate. Therefore, it appears that the inability of the aged APdE9 mice to release glutamate (upon stimulation) along with increased plaque burden may contribute to learning impairment in these mice.

## Materials and methods

### Animals

The APPswe/PS1dE9 (APdE9) founder mice were obtained from Johns Hopkins University, Baltimore, MD, USA (D. Borchelt and J. Jankowsky, Department of Pathology) and a colony was established at the University of Kuopio. These mice were generated by co-injection of chimeric mouse/human APPswe (mouse APP695 harboring a human A $\beta$  domain and mutations K595N and M596L linked to Swedish familial AD pedigrees) and human PS1-dE9 (deletion of exon 9) vectors controlled by independent mouse prion protein promoter elements (Jankowsky *et al.* 2004). This line was originally maintained in a hybrid C3HeJ x C57BL6/J F1 background, but the mice used in the present study were derived from backcrossing to C57BL6/J for 5–6 generations. The housing conditions (National Animal Center, Kuopio, Finland) were controlled (temperature +22°C, light from 07:00 to 19:00; humidity 50–60%), and fresh food and water were freely available. The experiments were conducted according to the Council of Europe (Directive 86/609) and Finnish guidelines, and approved by the State Provincial Office of Eastern Finland.

### Behavioral testing

Three separate groups of male APdE9 mice and their wild-type littermates (WT) were tested in Morris water maze to assess age-dependent memory impairment. The group sizes and age were as follows: 6 months: WT ( $n = 12$ ), APdE9 ( $n = 13$ ); 10 months: WT

( $n = 15$ ), APdE9 ( $n = 19$ ); 15 months: 20 WT ( $n = 20$ ), APdE9 ( $n = 19$ ). The apparatus was a black plastic pool with a diameter of 120 cm located in a well-lit room. A black escape platform (square, 14 cm  $\times$  14 cm) was located 1.0 cm below the water surface and was invisible to the mouse because of the light reflection from the water surface. The temperature of the water was kept constant throughout the experiment ( $20 \pm 0.5^\circ\text{C}$ ), and a 10-min recovery period was allowed between the training trials. First, the mice were pre-trained to find and climb onto the platform for two days by using an alley (1 m  $\times$  14 cm  $\times$  25 cm) leading to platform located 1 cm below the water. The test for the task acquisition consisted of four consecutive days of testing, with five trials per day, each 60 s. If the mouse failed to find the escape platform within the maximum time (60 s), it was placed there for 10 s by the experimenter. The platform location was kept constant and the starting position varied between four constant locations at the pool rim. Mice were placed in the water with their nose pointing towards the wall at one of the starting points in a random manner. On the 5th trial of Day 4, the platform was removed and the mice were allowed to swim for 60 s to determine their search bias.

The timing of the latency to find the submerged platform was started and ended by the experimenter. A computer connected to an image analyzer (HVS Image®, Hampton, UK) monitored the swim pattern. During the water maze training we measured the swimming speed and latency to find platform. The search bias during the probe trial was measured by calculating the time the mice spent in the vicinity of the former platform position. We defined this as a target area centered on the platform and with a diameter of 30 cm. This target area comprised 6.25% of the total surface area, thus a random swim for 60 s in the pool would yield a dwell time of 3.75 s in the target area during the probe trial.

### Microdialysis

Female young adult (7 months) WT ( $n = 8$ ) and APdE9 ( $n = 9$ ) mice and middle-aged (17 months) WT ( $n = 8$ ) and APdE9 ( $n = 6$ ) mice were used in the microdialysis study.

Under pentobarbital-chloralhydrate anesthesia, the guide cannula (CMA, Stockholm, Sweden) was stereotactically implanted in the right hippocampus at the following coordinates (mm from bregma: A  $-3.1$ , L  $+2.8$ , V  $-2.0$ ). One week post-surgery and the day before the actual dialysis experiment, the microdialysis probe (diameter 0.24 mm, CMA/7, Stockholm, Sweden) was inserted through the guide cannula, and the hippocampus was continuously perfused with the Ringer solution (145 mmol/L NaCl, 2.7 mmol/L KCl, 1.2 mmol/L CaCl<sub>2</sub>, and 1.0 mmol/L MgCl<sub>2</sub>) at a rate of 0.5  $\mu\text{L}/\text{min}$  for 18 h (CMA/100 Microinjection Pump, Solna, Sweden). The next day, the perfusion speed was increased to 2  $\mu\text{L}/\text{min}$  and the perfusion was continued for the next 2 h before sampling the dialysate. The total sampling time was 3 h 40 min and included 22 samples (each 10 min). First, five baseline samples were collected (50 min). Then the perfusion fluid was switched from normal Ringer to high KCl-Ringer containing 25 mmol/L KCl to depolarize the neurons. Three subsequent samples (30 min) were collected to capture the stimulated glutamate release. This was followed by the collection of eight baseline samples (80 min). In order to determine the origin of the released transmitter, a second KCl stimulation (30 min) was given in the presence of 1  $\mu\text{mol}/\text{L}$  tetrodotoxin (TTX). Finally, the perfusion was continued for 30 min

with 1  $\mu\text{mol}/\text{L}$  TTX alone to block glutamate release based on neuronal activity.

At the end of the experiment, the mouse was deeply anesthetized with pentobarbiturate-chloralhydrate cocktail (60 mg/kg each) and perfused with 50 mL heparinized ice-cold 0.9% saline (10 mL/min), after which the brains were rapidly removed. One hemibrain was immersed in 4% paraformaldehyde in 0.1 mol/L Na-phosphate buffer for 4 h, and then transferred to a 30% sucrose solution overnight and finally stored in a cryoprotectant in  $-20^\circ\text{C}$  for later immunohistology. The other hemibrain was dissected on ice into selected brain areas (hippocampus, ventral and dorsal cortexes) that were stored in  $-70^\circ\text{C}$  for biochemical assays.

### Analysis of dialysates for glutamate

Analysis of amino acid samples occurred by reversed phase HPLC (A1100, Agilent, Amsterdam, the Netherlands) with a separate column heater (Mistral; Spark, Emmen, the Netherlands) and a fluorescence detector (Jasco FP-920 FLDetector, Separations, H.I.Ambacht, the Netherlands). Data were acquired and analyzed by Empower software (Waters Corporation, Milford, MA, USA, USA) on a workstation computer.

For pre-column derivatization, 12  $\mu\text{L}$  of biological sample was mixed 1 : 1 with the derivatizing agent ( $\beta$ -mercapto-ethanol in an *o*-phthaldialdehyde (OPA) solution) in the injection needle. After pre-column derivatization the dialysis samples were automatically injected onto a Supelcosil™ LC-18DB reversed-phase column (150 mm  $\times$  4.6 mm; dp = 3  $\mu\text{m}$ ; Supelco, PA, USA). The flow rate was set at 1.0 mL/min, and gradient elution was used during the run in order to obtain optimal separation of compounds and also to clean the column before the injection of the next sample. Elution buffer was a 7.4 mol/L MeOH containing 0.1 mol/L Na<sub>2</sub>HPO<sub>4</sub> and 2.1 mmol/L Na<sub>2</sub>EDTA with pH adjusted to 6.4. The column was maintained at a constant temperature of 15°C with a column oven. The end of the column was coupled to a fluorescence detector with excitation and emission wavelengths set at 325 and 418 nm, respectively. The retention time of glutamate was 2.88 min with respective detection limit of 0.52 nmol/L. All samples were run in an ordered-random sequence with standard solutions (5.2  $\mu\text{mol}/\text{L}$  of glutamate dissolved in 0.1 mol/L trichloric acid) being injected before and after every eight samples.

### Analysis of hippocampal A $\beta$ levels

A $\beta$ 1–40 and A $\beta$ 1–42 levels were determined from hippocampal samples of separate groups of male APdE9 mice at ages of 6 ( $n = 5$ ), 9 ( $n = 12$ ) and 16 ( $n = 10$ ) months. The tissue was homogenized on ice in 7 volumes of 20 mmol/L Tris-HCl buffer, pH 8.5, containing a cocktail of protease inhibitors (COMPLETE™, Roche Diagnostics, Basel, Switzerland; Marutle *et al.* 2002). After centrifugation (50 000 *g* for 1 h at 4°C), the supernatant was diluted 1 : 1 with phosphate-buffered saline (PBS) including 0.5% bovine serum albumin, 0.05% Tween 20 and the cocktail of protease inhibitors (PBS) buffer, and used for analysis of soluble A $\beta$ 1–40 and A $\beta$ 1–42. The pellet was resuspended and extracted in 8 volumes of 5 mol/L guanidium-HCl in 50 mmol/L Tris-HCl, pH 8.0, for 4 h at room temperature (22°C). This extract was centrifuged at 40 000 *g* for 20 min at 4°C. The supernatant was further diluted with PBS buffer 1 : 50 before the assay. The levels of A $\beta$ 1–40 and A $\beta$ 1–42

were analyzed by a colorimetric sandwich ELISA kits (Signal Select™ Human  $\beta$  Amyloid 1–40 and 1–42 kits, BioSource International Inc., Camarillo, CA, USA). The assay was performed according to the manufacturer's protocol and values were calculated by comparison with standard curves made by using synthesized hA $\beta$ 1–40 and 1–42, respectively. The absorbance at 450 nm was determined using a Multiscan® MS microplate spectrophotometer (Thermo Fisher Scientific, Waltham, MA, USA). Final values of A $\beta$ 1–40 and A $\beta$ 1–42 in the brain were expressed as pg/mg wet weight tissue.

#### Analysis of glutamate transporters, synaptophysin and GFAP levels

Brain homogenates of the very same mice that were involved in the microdialysis experiment were used in immunoblotting. An additional group of 5- and 14-month-old mice (6 APdE9 and 6 wt in each age group) were used to harvest hippocampal tissue for GFAP immunoblotting. Brain samples were diluted 1 : 10 in the sample buffer, and the volumes were adjusted between 10–15  $\mu$ l to contain equal amounts of  $\beta$ -actin, determined in a separate immunoblotting experiment. The samples were loaded onto 10% sodium dodecyl sulfate–polyacrylamide gel electrophoresis mini-gels and electrophoresed in Mini-Protean 3 (Bio-Rad, Hercules, CA, USA) for 40 min at 200 V constant voltage. After electrophoresis, proteins were transferred on polyvinylidene difluoride Hybond membrane (GE Healthcare, Amersham, UK) at constant 380 mA for 1 h at 4°C in Mini Trans-Blot Electrophoretic Transfer Cell (Bio-Rad, Hercules, CA, USA). The membranes were blocked with 5% skimmed milk in PBS containing 0.2% Tween 20 for 30 min at 22°C.

The primary detection antibodies and their dilutions were as follows: anti-VLUT1, Synaptic Systems (Goettingen, Germany), 1 : 2000; anti-VGLUT2, Synaptic Systems, 1 : 2000; anti-GLT-1, Calbiochem (San Diego, CA, USA), 1 : 1000; anti-synaptophysin, Synaptic Systems, 1 : 2000; anti-GFAP, Dako (Cambridgeshire, UK), 1 : 1000. The primary antibodies were diluted in 5% milk/PBS-T and let to incubate overnight at 4°C. Anti-rabbit IgG, horseradish peroxidase-linked whole antibody (GE Healthcare) was used as the secondary antibody (dilution 1 : 2800 in 5% milk/PBS-T, incubation 2 h at 22 °C). The immunoblots were developed with ECL plus western blotting Detection System (GE Healthcare) and scanned with STORM860 scanner. The results were analyzed with ImageQuaNT-program.

#### Immunohistochemistry

The immersion fixed hemibrains of mice involved in the microdialysis experiment were cut on sliding/freezing microtome into 35  $\mu$ m coronal sections for the determination of the probe location in cresyl violet-stained sections. In addition, the brains were stained for human A $\beta$  selective 6E10 antibody (Senetec, St Louis, MO, USA) for visualizing amyloid plaques.

A separate group of male 6-month-old APdE9 ( $n = 5$ ) and wild-type ( $n = 5$ ) and 16-month-old APdE9 ( $n = 10$ ) and wild-type ( $n = 7$ ) mice were anesthetized with pentobarbital and perfused with heparinized saline (5000 IU/L). The brains were dissected out and the right hemisphere was immersion fixed with freshly prepared 4% paraformaldehyde for overnight at 4°C. After cryoprotection in 30% sucrose for 48 h the brains were frozen on liquid nitrogen and stored at –80°C. (Hippocampi from the left hemisphere were dissected out for determination of A $\beta$  concentrations and snap frozen on liquid

nitrogen). Immunohistochemistry was performed on 20  $\mu$ m thick cryostat sections using an antibody recognizing astrocytic GFAP (1 : 500, Dako). Following overnight incubation with GFAP antibody, the sections were reacted against biotinylated secondary antibody (1 : 200 dilution, Vector Laboratories, Peterborough, UK), and avidin-biotin complex (Vectastain Elite Kit, Vector Laboratories) according to manufacturer's instructions. Immunoreactivity was visualized with H<sub>2</sub>O<sub>2</sub> and nickel-enhanced diaminobenzidine. In selected cases, the sections were further stained with congo red to visualize the location of GFAP positive astrocytes with regard to plaque cores. The sections were imaged with Olympus AX70 microscope (Olympus-Europa, Hamburg, Germany) under appropriate sets of filters with an attached digital camera (Color View 12 or F-View, Soft Imaging System, Munster, Germany) running an Analysis Software (Soft Imaging System). Quantification was done from 4–6 sections through hippocampi using ImagePro Plus software (Media Cybernetics, Silver Spring, MD, USA). Data are expressed as a percentage of immunoreactive area in hippocampi and represented as the mean  $\pm$  SEM.

#### Statistics

All statistical analyses were performed using SPSS for Windows 11.0 software (SPSS Inc, Chicago, IL, USA). The water maze acquisition data were analyzed using ANOVA for repeated measures, with the test day as the within-subject factor. In addition, the search bias in the target area was compared between the genotypes by using Student's *t*-test. The baseline and KCl-evoked glutamate levels (the mean of three sampled during the first KCl stimulation) between the two ages and two genotypes were analyzed using ANOVA with age and genotype as factors. The number of responders and non-responders to KCl stimulation in each group was compared with Fisher's exact test. The levels of glutamate transporters, synaptophysin and GFAP were analyzed with ANOVA with age and genotype as factors.

## Results

### Spatial learning and memory

We tested 13 APdE9 male mice and their 12 non-transgenic littermates in the water maze at 6 months of age. No difference was found in their escape latency ( $F(1, 23) = 0.5$ ,  $p = 0.48$ ; Fig. 1a) or swimming speed ( $F(1, 23) = 0.4$ ,  $p = 0.85$ ). In the probe test conducted on the 5th trial of Day 4, both APdE9 and control mice showed a normal search bias at the former platform location (Fig. 1d), ( $t_{21} = 0.4$ ,  $p = 0.72$ ). Another set of 19 male APdE9 mice and their 15 non-transgenic littermates were tested at the age of 10 months. At 10 months, the APdE9 mice displayed a moderate deficiency in their escape latency [ $F(1, 32) = 3.7$ ,  $p = 0.06$ ; Fig. 1b], but they did not differ from the control mice in the swimming speed [ $F(1, 32) = 0.5$ ,  $p = 0.47$ ]. In the probe test the control mice showed a normal search bias at the former platform location (Fig. 1e), whereas APdE9 mice failed to show such a bias ( $t_{32} = 1.9$ ,  $p = 0.07$ ). Finally, we tested 19 male APdE9 mice with their 20 non-transgenic

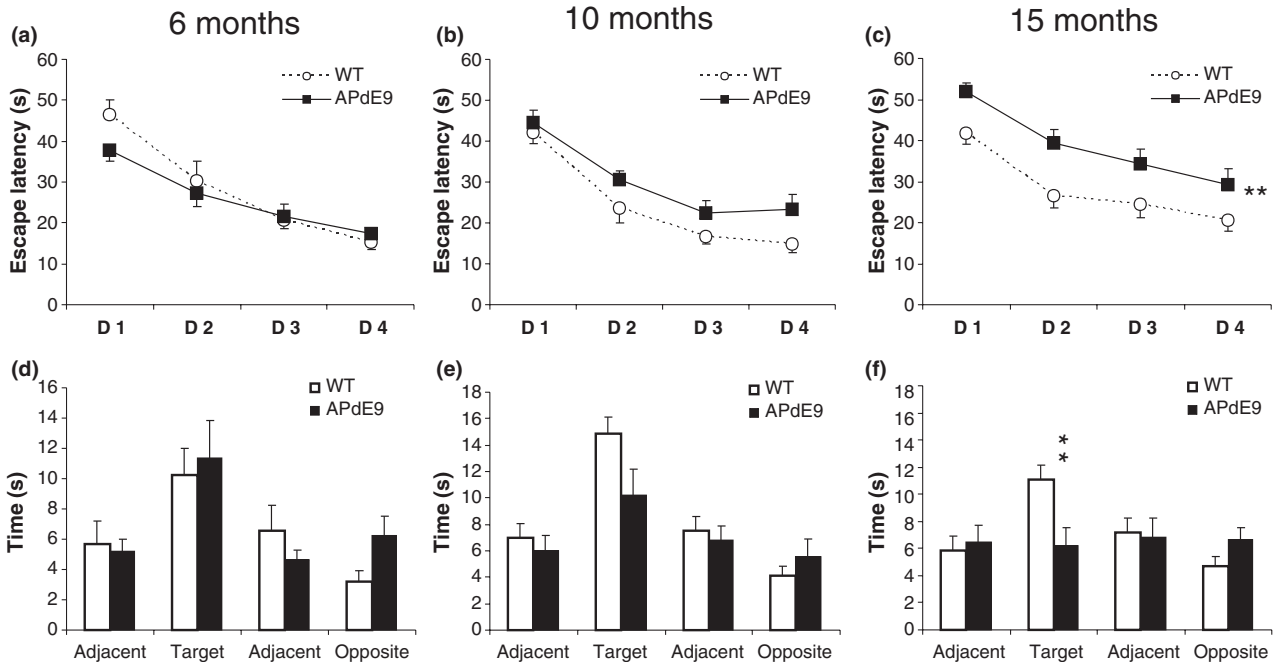


**Fig. 1** Age-related impairment in spatial learning and memory in APdE9 mice. (a–c) Acquisition of the water maze task during five daily trials over four days (D1–D4). Group means  $\pm$  SEM are shown for the escape latency to the hidden platform. (d–f). A 60-s probe trial for

search bias was conducted on the last trial on Day 4. Time spent in a near vicinity of the previous platform location (target) on three other corresponding locations symmetrically around the pool is given. \*\*Significant difference between the genotypes,  $p < 0.01$ .

littermates at 15 months of age. At this age, APdE9 mice exhibited significant impairment in the escape latency ( $F(1, 37) = 12.6, p = 0.001$ ; Fig. 1c), although they did not differ in their swimming speed from their non-transgenic counterparts [ $F(1, 37) = 3.3, p = 0.08$ ]. In the probe test on Day 4, the control mice showed a normal search bias at the former platform location (Fig. 1f), whereas APdE9 mice failed to show such a bias ( $t(37) = 2.8, p < 0.01$ ). These data indicate that the impairment in spatial memory in APdE9 mice developed gradually between the ages 6 and 15 months.

### Hippocampal glutamate levels

The number of animals that yielded acceptable microdialysis samples was as follows: 7-month-old wild-type ( $n = 8$ ) and APdE9 ( $n = 9$ ), 17-month-old wild-type ( $n = 8$ ) and APdE9 ( $n = 6$ ). One young APdE9 mouse and two aged wild-type mice exhibited very high KCl-stimulated glutamate levels (above 2 SDs of the group mean). These animals were excluded from the group means as outliers. However, they were included in the number of animals responding to the KCl stimulation. Figure 2 illustrates fluctuations in the extracellular glutamate levels during the course of the experiment. Notably, glutamate levels returned to baseline after the first KCl stimulation speaking against any sustained damage because of the stimulation. Moreover, when a second KCl stimulation was given for 30 min in the presence of TTX, it led to only a marginal glutamate release, suggesting

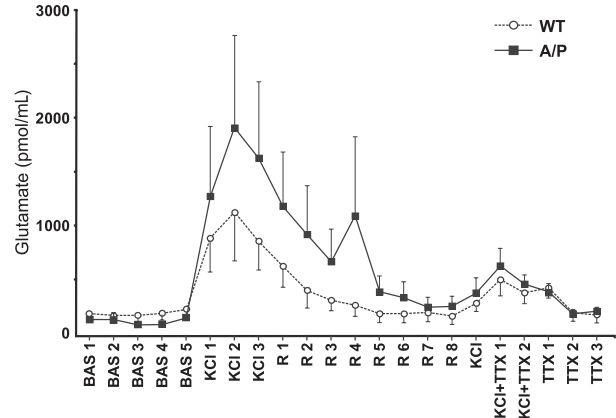


**Fig. 2** Effect of KCl stimulation and TTX on glutamate release in the hippocampus of 7-month-old APdE9 ( $n = 8$ ) and control ( $n = 8$ ) mice. BAS, baseline; KCl, stimulation with potassium chloride; R, recovery with normal Ringer perfusion; TTX, tetrodotoxin. Each division of x-axis corresponds to 10 min sampling. Group means  $\pm$  SEM are given for each 10-min sample.

that during the first stimulation glutamate derives from TTX-sensitive, excitable cells.

The ANOVA revealed an age-dependent decline in stimulated (first KCl stimulation) glutamate levels in both APdE9 and non-transgenic mice ( $F(1, 24) = 5.2, p = 0.03$ ). However, there was no genotype effect ( $p = 0.99$ ) or age by

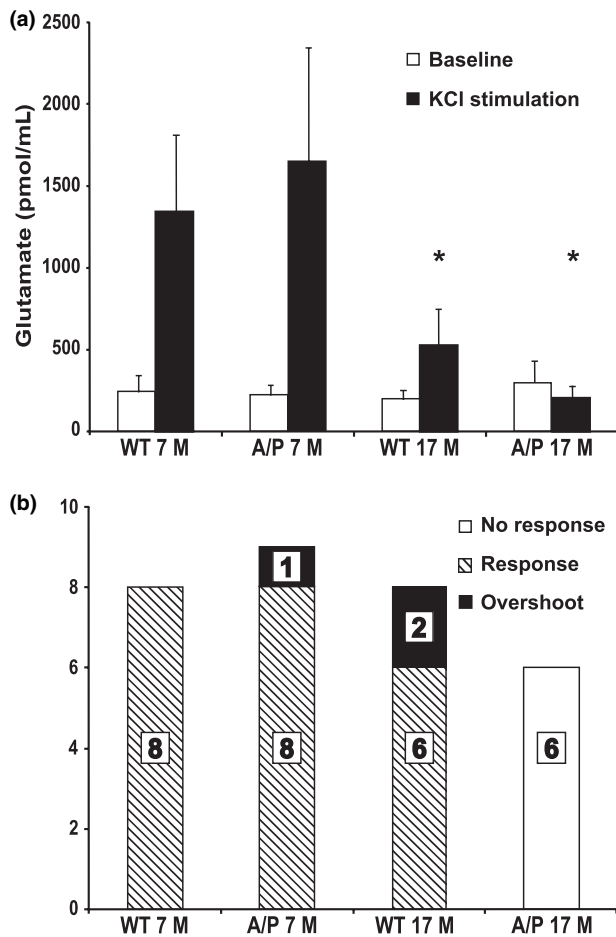


**Fig. 3** Summary of glutamate release in APdE9 and control mice at 7 and 17 months of age. (a) Baseline and peak glutamate release (pmol/mL) in each of the four groups (mean  $\pm$  SEM). \*Significant age-related decline,  $p < 0.05$ . (b) Percentage of mice in each group with a 25% increase in glutamate release from baseline after KCl stimulation. Number of animals in each group: 7-month-old wild-type ( $n = 8$ ) and APdE9 ( $n = 8 + 1$ ); 17-month-old wild-type ( $n = 6 + 2$ ) and APdE9 ( $n = 6$ ). Hatched columns = response to KCl stimulation, filled columns = response overshoot, excluded from the group means as statistical outliers, open columns = no response to KCl stimulation.

genotype interaction ( $p = 0.53$ ) (Fig. 3a). In contrast, the baseline glutamate levels were not influenced by age or by genotype ( $p = 0.36$ ). Because the absolute peak glutamate levels varied greatly between individual animals, which may have obscured significant group differences, we also analyzed the data by comparing the response to KCl stimulation with individual baseline levels. Mice showing a 25% increase or greater from baseline in response to KCl stimulation were classified as responders, while those showing a smaller change were classified as non-responders. Using this criterion, all APdE9 and wild-type young animals were responders. By contrast, none of the middle-aged APdE9

mice responded to KCl, although all middle-aged wild-type mice were responders. This difference in KCl response between middle-aged APdE9 and wild-type mice was statistically significant ( $p = 0.002$ , Fisher's exact test). This difference in KCl response became even more drastic when the two excluded middle-aged wild-type mice exhibiting very high peak glutamate levels were taken into account (Fig. 3b). Histology verified that the probe was in contact with the hippocampus in all mice, and that the difference between responders and non-responders cannot be attributed to the probe location.

### Glutamate transporters and synaptophysin-1

Hippocampal tissue samples from the mice used for microdialysis were used to determine the levels of glutamate transporters and synaptophysin.  $\beta$ -actin normalized levels of VGLUT1 showed an age-dependent decline ( $F(1, 24) = 4.4$ ,  $p < 0.05$ ) (Fig. 4a and c), but there was no genotype difference ( $p = 0.69$ ) or age by genotype interaction ( $p = 0.58$ ). Although VGLUT2 levels tended to change with age in APdE9 mice (Fig. 4b and d), neither age ( $p = 0.25$ ) nor genotype ( $p = 0.48$ ) effect reached significance. Unlike VGLUT, the levels of GLT-1 did not change with age or genotype (Fig. 4e and g). The hippocampal levels of synaptophysin-1 showed a trend towards age-dependent decline ( $F(1, 24) = 3.8$ ,  $p = 0.07$ ; Fig. 4f and h), but there was no genotype difference or age by genotype interaction.

### GFAP levels

We also tested the possibility that the observed decrease in KCl-evoked glutamate levels in the hippocampus of middle-aged APdE9 mice may have been due to increased number of astrocytes, which could effectively clear glutamate from the extracellular space. To do this, a separate group of male APdE9 (6 months,  $n = 5$ ; 16 months,  $n = 10$ ) and wild-type mice (6 months,  $n = 5$ ; 16 months,  $n = 7$ ) were perfused, and their coronal brain sections were stained for GFAP. The GFAP immunoreactive area in the hippocampus tended to increase with age ( $F(1, 22) = 3.7$ ,  $p = 0.07$ ), but there was no age by genotype interaction ( $p = 0.40$ ) (Fig. 5c). However, apart from a general increase in the GFAP positive area with age in APdE9 mice also the GFAP staining pattern changed, such that in middle-aged mice the GFAP positive astrocytes were clearly concentrated around the plaques (Fig. 5b and e). Because immunoreactive surface area does not take into account possible intensity differences in pixels passing the set threshold, it is not a particularly sensitive measure to a local increase in the GFAP signal around the plaques. Therefore, an additional group of male APdE9 (5 months,  $n = 6$ ; 14 months,  $n = 6$ ) and wild-type mice (5 months,  $n = 6$ ; 14 months,  $n = 6$ ) were used to harvest fresh hippocampal samples for western blotting to obtain another measure of GFAP levels. In this set of samples, actin-normalized GFAP levels increased with age in APdE9 mice

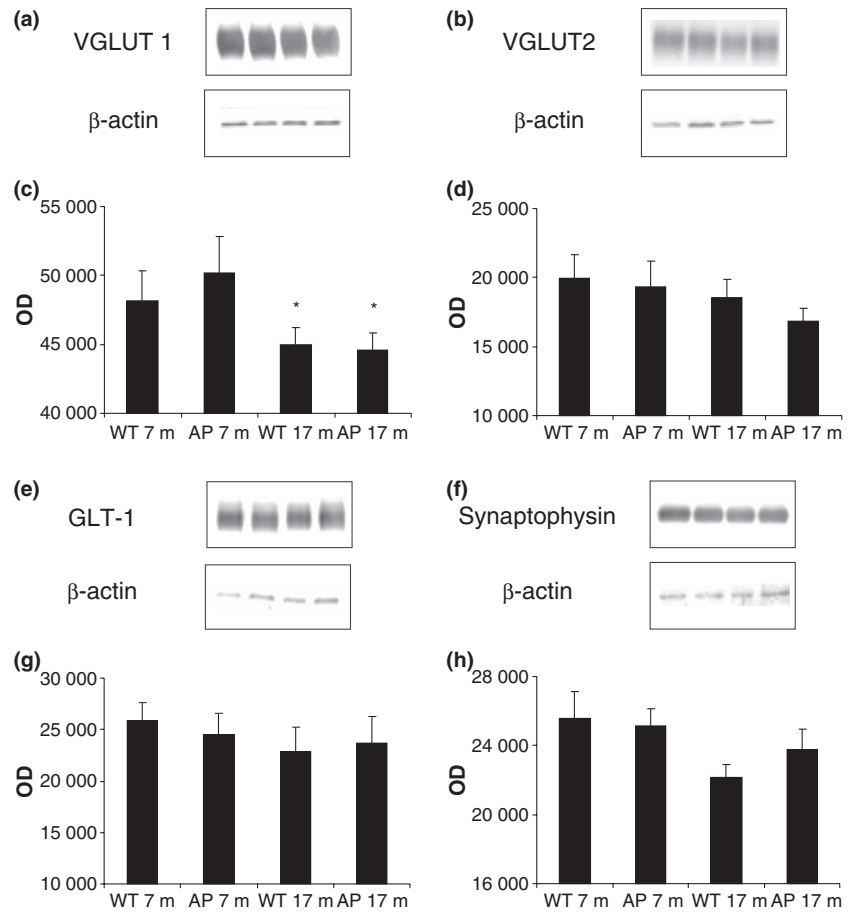


**Fig. 4** Immunoblots for the determination of VGLUT1, VGLUT2, synaptophysin and GLT-1 levels. Bands from the Western blot of individual animals are shown for VGLUT1 (a), VGLUT2 (b), GLT-1 (e) and synaptophysin (f) in the following order: 1 = WT 7 m, 2 = A/P 7 m, 3 = WT 17 m, 4 = A/P 17 m. Mean optic densities ( $\pm$  SEM) are also shown for VGLUT1 (c), VGLUT2 (d), GLT-1 (g) and synaptophysin (h) levels. \*Significant age-related decline,  $p \leq 0.05$ .

but not in their wild-type littermates (Fig. 5d and f), which resulted in a significant age  $\times$  genotype interaction ( $F(1,20) = 5.8$ ,  $p = 0.03$ ).

### $\beta$ -Amyloid levels

We measured brain A $\beta$  plaques using 6E10 antibody in the brain sections prepared from mice that underwent microdialysis. Additionally, the brain tissue levels of soluble and insoluble A $\beta$ 40 and A $\beta$ 42 were determined in a separate group of 6-month-old ( $n = 5$ ), 9-month-old ( $n = 9$ ) and 16-month-old APdE9 mice ( $n = 10$ ). As described before (Savonenko *et al.* 2005), both soluble and insoluble A $\beta$  levels rose steeply with age (Fig. 6a and b). The increase was much greater for the more amyloidogenic A $\beta$  1–42 than A $\beta$  1–40, and was accompanied by increasing formation of amyloid plaques. Although the hippocampus had only a few amyloid plaques at 6 months of age, the above lying cortex displayed substantial amyloid burden already at this age (Fig. 6c and e).

### Discussion

The present study showed that spatial memory impairment in APdE9 mice occurs between 10 and 15 months of age, while

substantial amount of amyloid plaques are present in the cortex and hippocampus in these mice already at 6 months of age. Although the continued increase in the brain A $\beta$  load from 10 to 15 months may partially account for the rapid deterioration of spatial memory in APdE9 mice, other factors specific for this age range are more likely to account for the rapid memory decline. Therefore, we wanted to determine possible changes in glutamatergic neurotransmission in APdE9 and wild-type mice younger and older than this age range. We found a selective decrease in KCl-stimulated glutamate release in the hippocampus of 17-month-old APdE9 mice compared to the 7-month-old APdE9 mice; the basal glutamate levels did not change significantly between the two age groups. Although a similar age-related decline in KCl-stimulated glutamate release was also observed in wild-type mice it was much less dramatic. Supporting this, a recent study on mice carrying the same APdE9 mutations demonstrated moderately increased KCl-stimulated glutamate release in 3-month-old APdE9 mice but significantly decreased release compared to wild-type littermates at 10 months of age (Jorgensen *et al.* 2007). These findings suggest that blunted stimulated glutamate release in aged APdE9 mice likely contributes to age-related spatial memory impairment in these mice.

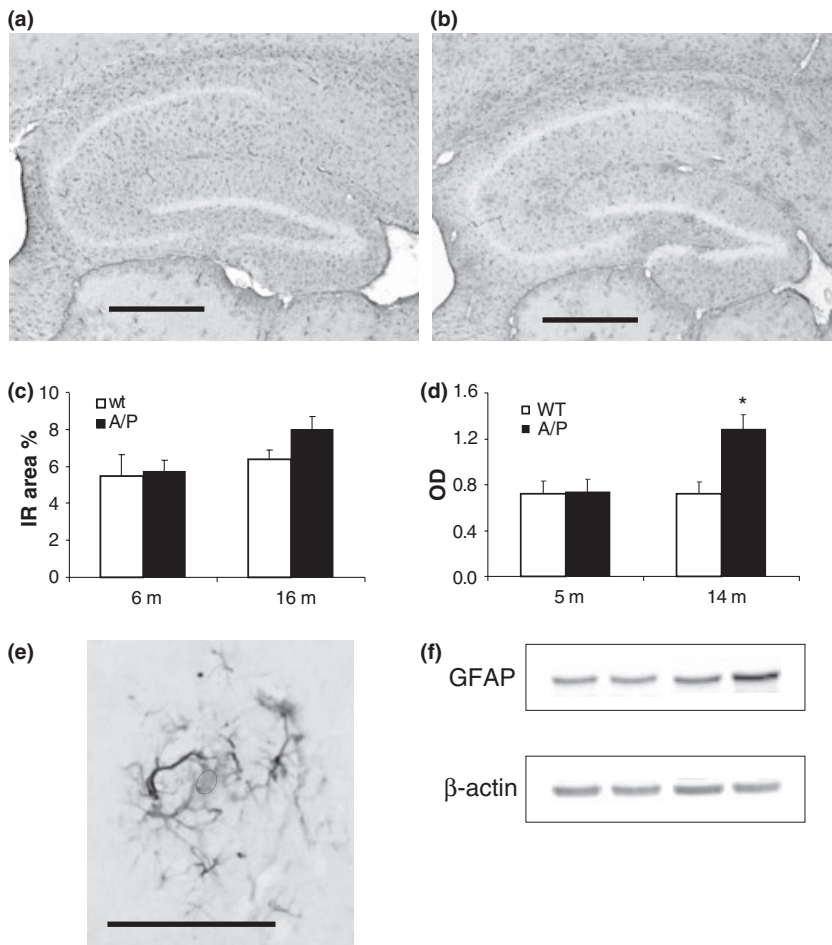


**Fig. 5** Age-related changes in glial fibrillary acidic protein (GFAP) levels in the hippocampus. A representative coronal section through the septal hippocampus of a 16-month-old wild-type (a) and an APdE9 mouse (b). Scale bar = 500  $\mu$ m. (c) Group means  $\pm$  SEMs for the immunopositive area as % of total surface area. No significant group differences were found. (d) GFAP levels normalized to  $\beta$ -actin in a western blot from the hippocampus of 5- and 14-month-old wild-type and APdE9 mice. \*The aged APdE9 mice differ significantly from all other groups (Tukey HSD,  $p = 0.01$ ). (e) Double staining for GFAP and Congo red demonstrating the accumulation of GFAP positive astrocytes around the amyloid plaque core (circled to enhance the contrast in the b/w image). Scale bar: 50  $\mu$ m. (f) Representative bands from the GLT-1 western blot of individual animals are shown in the same order as the groups in panel D: 1 = WT 5 m, 2 = A/P 5 m, 3 = WT 14 m, 4 = A/P 14 m.

### Age-related changes in transmitter versus metabolic pool of glutamate

Our finding of unchanged basal glutamate levels with aging combined with blunted glutamate release in response to  $K^+$  stimulation appears at odds with the existing literature (Segovia *et al.* 2001). However, it is worth noticing that glutamate measured with different methods may actually reflect levels of glutamate in different pools. The extracellular glutamate concentration, which is estimated to be 1  $\mu$ mol/L at most, is also a minute fraction of the total cellular glutamate concentration, which in neurons is estimated to be around 5 mmol/L and in astrocytes 2–3 mmol/L (Nedergaard *et al.* 2002). Furthermore, 70–80% of glutamate in neurons is estimated to reside in the metabolic pool and only 20–30% in glutamatergic nerve terminals (Fonnum 1993). So an age-related decline in glutamate concentration in tissue homogenates more likely reflects changes in the metabolic pool, such as reduced metabolic activity, than those of the neurotransmitter glutamate. In addition, any cellular damage, such as insertion of the probe, not to mention chopping of a brain block for slices, easily leads to substantial non-physiological leak of glutamate into the extracellular space. To avoid glutamate leak because of

cell injury, we implanted guide cannula into the brain a week before the probe insertion and also perfused the probe at slow flow rate overnight. To further separate neurotransmitter glutamate from metabolic one, we used KCl stimulation and TTX. Comparison of peak glutamate release in response to KCl stimulation in the absence and presence TTX clearly differed (Fig. 2), indicating that a substantial part of the measure glutamate release derives from excitable cells. However, this does not fully guarantee that the source of the glutamate is neuronal, as recent data indicate that astrocytes can also release glutamate from transmitter vesicles in response to increased cytosolic  $Ca^{2+}$  (Montana *et al.* 2006). Nevertheless, with all the precautions taken, the present study gives a better approximation of synaptic glutamate than the majority of earlier studies reporting age-related changes in released glutamate.

Only two studies to our knowledge have assessed age-related changes in glutamate release by using *in vivo* microdialysis, both of them in rats. Whereas one study in 24-month-old Fisher-344 rats (Zhang *et al.* 1991) reported about 30% reduction in extracellular glutamate concentration in the hippocampus of aged rats, another study found 60% increase in Wistar rats of similar age (Massieu and

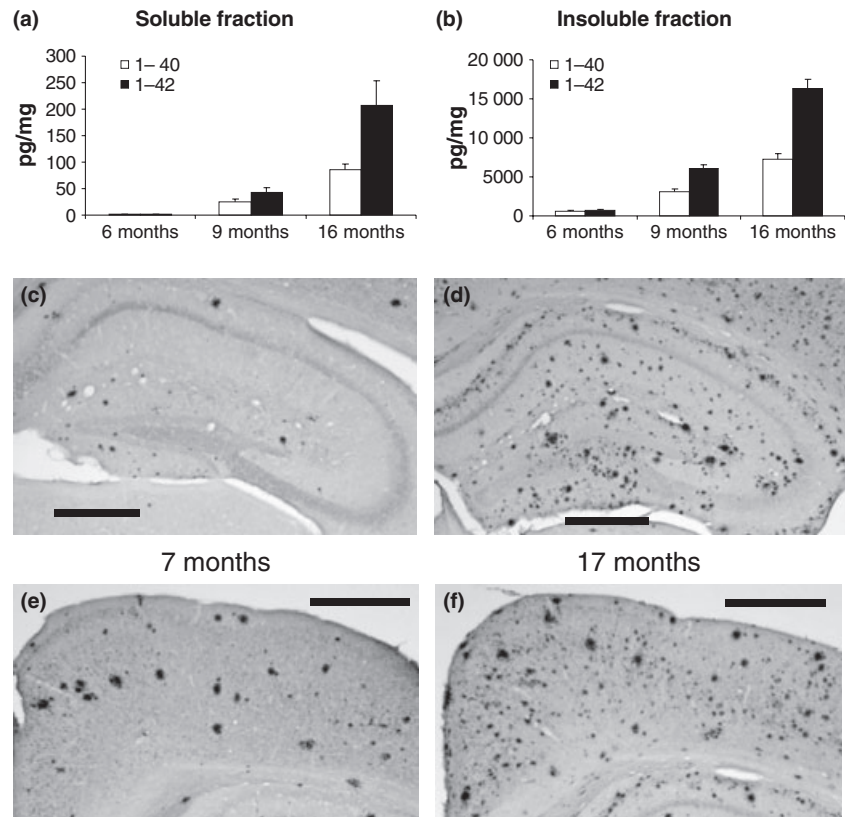


**Fig. 6** Development of amyloid pathology with age. Soluble (a) and insoluble (b) A $\beta$ 1-40 and 1-42 levels in APdE9 mice at 6, 9, and 16 months of age. Representative coronal sections through the septal hippocampus (c and d) and medial somatosensory cortex (e and f) of one 7- and one 17-month-old APdE9 mouse involved in the microdialysis experiment. Scale bar: 500  $\mu$ m.

Tapia 1997). Moreover, the latter study reported about 50% increase in stimulated glutamate release in aged animals, which is opposite to our finding. However, a number of methodological details are likely to explain these discrepant findings. Whereas we and Zhang *et al.* used freely moving animals, Massieu and Tapia used halothane anesthesia throughout the experiment. Maybe more importantly, they let the baseline stabilize only for 60 min after the probe insertion, while we and Zhang *et al.* perfused the tissue overnight. Finally, we used KCl to promote glutamate release through membrane depolarization, while Massieu and Tapia used a glutamate uptake blocker to increase extracellular glutamate levels (Massieu and Tapia 1997). It is clear that more experiments are needed before the issue of age-related changes in glutamate release can be settled.

#### Age-related decrease in glutamate transporter levels may not be sufficient to abolish stimulated glutamate release in APdE9 mice

The vesicular glutamate transporters have an important role in the release of glutamate from pre-synaptic vesicles (Wojcik *et al.* 2004; Wilson *et al.* 2005). In this study, determination of the tissue levels of vesicular glutamate transporter proteins VGLUT1 and VGLUT2 corroborated the finding of our microdialysis studies, showing by and large

similar age-dependent decrease in their levels as that of KCl-stimulated glutamate release. However, modestly lower levels of VGLUT1 and VGLUT2 in aged APdE9 mice compared to aged wild-type mice cannot account for the total lack of responsiveness to KCl stimulation in middle-aged APdE9 mice, but it requires additional deficits in the pre-synaptic terminals. One such mechanism may be altered response to KCl, e.g. because of the changes in the number or kinetics of K<sup>+</sup> channels. The APdE9 presenilin mutation itself has been shown to alter outward K<sup>+</sup> currents in cultured human cells, although the reports disagree as to whether the change is toward an increase (Malin *et al.* 1998) or decrease (Plant *et al.* 2002). Nevertheless, it is difficult to explain on the basis of the presenilin mutation why we see a slight increase in stimulated glutamate release in young adult APdE9 mice but a blunted response in aged ones. Therefore, consequences of A $\beta$  accumulation with aging fits better with the current observations. Depending on the cell type, concentration and special species or conformation of the peptide, A $\beta$  has been reported to either inhibit (Good *et al.* 1996; Ye *et al.* 2003) or augment (Plant *et al.* 2006) A-type K<sup>+</sup> channels or inhibit delayed rectifier K<sup>+</sup> channels (Etcheberrigaray *et al.*, 1994; Ye *et al.* 2003). Clearly, more research is needed to reveal the role of K<sup>+</sup> channel modulation by presenilin and A $\beta$  on glutamate release *in vivo*.

### Reduced extracellular glutamate levels in aged APdE9 mice cannot be attributed to increased glutamate uptake into astrocytes

In addition to reduced glutamate release from axon terminals, low levels of extracellular glutamate in aged APdE9 mice could result from more effective uptake of glutamate into astrocytes. In support of this notion, we found significant increase in hippocampal levels of GFAP, a marker of activated astrocytes. However, two observations in the present study disfavor this hypothesis. First, enhanced uptake to astrocytes should preferably decrease basal extracellular glutamate levels. In contrast, these were slightly elevated in aged APdE9 mice compared to wild-type littermates. Second, we found no significant change in total GLT-1 protein levels with age. Furthermore, it is noteworthy that the GFAP protein levels in middle-aged APdE9 mice showed a more robust increase than the GFAP immunoreactive surface area. This likely reflects the fact that most intensive GFAP expression was restricted to astrocytes in the near vicinity of amyloid plaques, which is characteristic of a local inflammatory reaction around the plaques. Such an inflammatory reaction in turn can compromise synaptic glutamate release through several mechanisms.

### Can altered hippocampal glutamate release underlie spatial memory impairment in APdE9 mice?

Since KCl-stimulated glutamate release declined age-dependently in both wild-type and APdE9 mice, one may question the relevance of altered glutamate release to the observed age-dependent impairment of spatial memory only in APdE9 mice. We think that this is a significant factor for several reasons. First, although the average levels of KCl-stimulated glutamate release indeed declined age-dependently in both genotypes, there was a striking genotype difference among the aged animals in the number of responders and non-responders to the stimulation. Second, in aged APdE9 the decline in KCl-stimulated glutamate release may have reached a critical level, while still being above the threshold in aged wild-type mice. Third, the combination of low releasable glutamate and high levels of A $\beta$  may be detrimental to memory. For instance, aged wild-type mice may compensate for the blunted pre-synaptic glutamate release by receptor-level changes post-synaptically, whereas the presence of high amounts of A $\beta$  prevents such changes in transgenic mice. In support of this notion, robust decrease in cortical post-synaptic alpha-amino-3-hydroxy-5-methyl-4-isoxazole propionic acid (AMPA) currents compared to those in wild-type mice has been observed in our APdE9 mice, as well as in slices of wild-type mice treated with exogenous A $\beta$  (Shemer *et al.* 2006).

### Conclusions

In conclusion, we found no evidence for age-related increase in extracellular glutamate nor reduction in astrocytic gluta-

mate transporter protein GLT-1 during an age range with rapid decline in hippocampus-dependent spatial task. Thus, we found no support for the notion that glutamate excitotoxicity underlies age-related memory impairment, at least in APdE9 mice. In contrast, our *in vivo* microdialysis data combined with analysis of VGLUT1 and VGLUT2 protein levels suggest that a significant decrease in stimulated glutamate release takes place in aged APdE9 mice during the age range when spatial memory deficit manifests in this mouse model. Similar deficit in stimulated glutamate release may also contribute to memory deficit in Alzheimer's disease in humans.

### Acknowledgments

We thank Pasi Miettinen for skillful assistance in immunohistology. The work was supported by Forest Laboratories Inc., Jersey City, NJ, USA.

### Disclosure statement

Drs. N. Leguit and J. Glennon are employees of Pharmaceuticals Research Laboratories, Weesp, The Netherlands; Dr P. Banerjee is an employee of Forest Laboratories Inc., Jersey City, NJ, USA.

### References

- Almeida C. G., Tampellini D., Takahashi R. H., Greengard P., Lin M. T., Snyder E. M. and Gouras G. K. (2005) Beta-amyloid accumulation in APP mutant neurons reduces PSD-95 and GluR1 in synapses. *Neurobiol. Dis.* **20**, 187–198.
- Bell K. F., de Kort G. J., Steggerda S., Shigemoto R., Ribeiro-da-Silva A. and Cuello A. C. (2003) Structural involvement of the glutamatergic presynaptic boutons in a transgenic mouse model expressing early onset amyloid pathology. *Neurosci. Lett.* **353**, 143–147.
- Cha J. H., Farrell L. A., Ahmed S. F., Frey A., Hsiao-Ashe K. K., Young A. B., Penney J. B., Locascio J. J., Hyman B. T. and Irizarry M. C. (2001) Glutamate receptor dysregulation in the hippocampus of transgenic mice carrying mutated human amyloid precursor protein. *Neurobiol. Dis.* **8**, 90–102.
- Davies P. and Maloney A. J. F. (1976) Selective loss of central cholinergic neurons in Alzheimer's disease. *Lancet* **2**, 1403.
- Etcheberrigaray R., Ito E., Kim C. S. and Alkon D. L. (1994) Soluble beta-amyloid induction of Alzheimer's phenotype for human fibroblast K<sup>+</sup> channels. *Science* **264**, 276–279.
- Fonnum F. (1993) Regulation of the synthesis of the transmitter glutamate pool. *Prog. Biophys. Mol. Biol.* **60**, 47–57.
- Good T. A., Smith D. O. and Murphy R. M. (1996) Beta-amyloid peptide blocks the fast-inactivating K<sup>+</sup> current in rat hippocampal neurons. *Biophys. J.* **70**, 296–304.
- Greenamyre J. T. and Young A. B. (1989) Excitatory amino acids and Alzheimer's disease. *Neurobiol. Aging* **10**, 593–602.
- Hsieh H., Boehm J., Sato C., Iwatsubo T., Tomita T., Sisodia S. and Malinow R. (2006) AMPAR removal underlies Abeta-induced synaptic depression and dendritic spine loss. *Neuron* **52**, 831–843.
- Hyman B. T., Van Hoesen G. W. and Damasio A. R. (1987) Alzheimer's disease: glutamate depletion in the hippocampal perforant pathway zone. *Ann. Neurol.* **22**, 37–40.

- Jankowsky J. L., Fadale D. J., Anderson J. *et al.* (2004) Mutant presenilins specifically elevate the levels of the 42 residue beta-amyloid peptide *in vivo*: evidence for augmentation of a 42-specific gamma secretase. *Hum. Mol. Genet.* **13**, 159–170.
- Jorgensen A. B., Dalby N. O., Mork A. and Veng L. M. (2007) Presynaptic glutamatergic changes in the APPsw/PS1dE9 mouse model of Alzheimer's disease. *Neurodegenerative Dis.* **4**(Suppl.1): 241.
- Kirvell S. L., Esiri M. and Francis P. T. (2006) Down-regulation of vesicular glutamate transporters precedes cell loss and pathology in Alzheimer's disease. *J. Neurochem.* **98**, 939–950.
- Li S., Mallory M., Alford M., Tanaka S. and Masliah E. (1997) Glutamate transporter alterations in Alzheimer disease are possibly associated with abnormal APP expression. *J. Neuropathol. Exp. Neurol.* **56**, 901–911.
- Lowe S. L., Bowen D. M., Francis P. T. and Neary D. (1990) Anteromedial cerebral amino acid concentrations indicate selective degeneration of glutamate-enriched neurons in Alzheimer's disease. *Neuroscience* **38**, 571–577.
- Machova E., Jakubik J., Michal P., Oksman M., Iivonen H., Tanila H. and Dolezal V. (2006) Impairment of muscarinic transmission in transgenic APPsw/PS1dE9 mice. *Neurobiol. Aging* **2006**, Nov–29.
- Malin S. A., Guo W. X., Jafari G., Goate A. M. and Nerbonne J. M. (1998) Presenilins upregulate functional K<sup>+</sup> channel currents in mammalian cells. *Neurobiol. Dis.* **4**, 398–409.
- Marutle A., Unger C., Hellström-Lindahl E., Wang J., Puoliväli J., Tanila H., Nordberg A. and Zhang X. (2002) Elevated levels of Abeta1-40 and Abeta1-42 do not alter the binding sites of nicotinic receptor subtypes in the brain of APPsw and PS1 double transgenic mice. *Neurosci. Lett.* **328**, 269–272.
- Masliah E., Alford M., Mallory M., Rockenstein E., Moechars D. and Van Leuven F. (2000) Abnormal glutamate transport function in mutant amyloid precursor protein transgenic mice. *Exp. Neurol.* **163**, 381–387.
- Massieu L. and Tapia R. (1997) Glutamate uptake impairment and neuronal damage in young and aged rats *in vivo*. *J. Neurochem.* **69**, 1151–1160.
- Montana V., Malarkey E. B., Verderio C., Matteoli M. and Parpura V. (2006) Vesicular transmitter release from astrocytes. *Glia.* **54**, 700–715.
- Nedergaard M., Takano T. and Hansen A. J. (2002) Beyond the role of glutamate as a neurotransmitter. *Nat. Rev. Neurosci.* **3**, 748–755.
- Plant L. D., Boyle J. P., Thomas N. M. *et al.* (2002) Presenilin-1 mutations alter K<sup>+</sup> currents in the human neuroblastoma cell line. *SH-SY5Y* **13**, 1553–1556.
- Plant L. D., Webster N. J., Boyle J. P., Ramsden M., Freir D. B., Peers C. and Pearson H. A. (2006) Amyloid beta peptide as a physiological modulator of neuronal 'A'-type K<sup>+</sup> current. *Neurobiol. Aging* **27**, 1673–1683.
- Procter A. W., Palmer A. M., Francis P. T., Lowe S. L., Neary D., Murphy E., Doshi R. and Bowen D. M. (1988) Evidence of glutamatergic denervation and possible abnormal metabolism in Alzheimer's disease. *J. Neurochem.* **50**, 790–802.
- Savonenko A., Xu G. M., Melnikova T., Morton J. L., Gonzales V., Wong M. P., Price D. L., Tang F., Markowska A. L. and Borchelt D. R. (2005) Episodic-like memory deficits in the APPsw/PS1dE9 mouse model of Alzheimer's disease: relationships to beta-amyloid deposition and neurotransmitter abnormalities. *Neurobiol. Dis.* **18**, 602–617.
- Segovia G., Porras A., Del Arco A. and Mora F. (2001) Glutamatergic neurotransmission in aging: a critical perspective. *Mech. Ageing Dev.* **122**, 1–29.
- Shemer I., Holmgren C., Min R. *et al.* (2006) Non-fibrillar beta-amyloid abates spike-timing-dependent synaptic potentiation at excitatory synapses in layer 2/3 of the neocortex by targeting postsynaptic AMPA receptors. *Eur. J. Neurosci.* **23**, 2035–2047.
- Terry R. D., Masliah E., Salmon D. P., Butters N., DeTeresa R., Hill R., Hansen L. A. and Katzman R. (1991) Physical basis of cognitive alterations in Alzheimer's disease: synapse loss is the major correlate of cognitive impairment. *Ann. Neurol.* **30**, 572–580.
- Wilson N. R., Kang J., Hueske E. V., Leung T., Varoqui H., Murnick J. G., Erickson J. D. and Liu G. (2005) Presynaptic regulation of quantal size by the vesicular glutamate transporter VGLUT1. *J. Neurosci.* **25**, 6221–6234.
- Wojcik S. M., Rhee J. S., Herzog E., Sigler A., Jahn R., Takamori S., Brose N. and Rosenmund C. (2004) An essential role for vesicular glutamate transporter 1 (VGLUT1) in postnatal development and control of quantal size. *Proc Natl. Acad. Sci. USA* **101**, 7158–7163.
- Wong T. P., Debeir T., Duff K. and Cuello A. C. (1999) Reorganization of cholinergic terminals in the cerebral cortex and hippocampus in transgenic mice carrying mutated presenilin-1 and amyloid precursor protein transgenes. *J. Neurosci.* **19**, 2706–2716.
- Ye C. P., Selkoe D. J. and Hartley D. M. (2003) Protofibrils of amyloid beta-protein inhibit specific K<sup>+</sup> currents in neocortical cultures. *Neurobiol. Dis.* **13**, 177–190.
- Zhang W. Q., Mundy W. R., Thai L., Hudson P. M., Gallagher M., Tilson H. A. and Hong J. S. (1991) Decreased glutamate release correlates with elevated dynorphin content in the hippocampus of aged rats with spatial learning deficits. *Hippocampus* **1**, 391–397.
- Zoia C., Cogliati T., Tagliabue E., Cavaletti G., Sala G., Galimberti G., Rivolta I., Rossi V., Frattola L. and Ferrarese C. (2004) Glutamate transporters in platelets: EAAT1 decrease in aging and in Alzheimer's disease. *Neurobiol. Aging* **25**, 149–157.